Available online at www.sciencedirect.com

ScienceDirect

Scripta Materialia 57 (2007) 229–232

Scripta MATERIALIA

www.elsevier.com/locate/scriptamat

Compaction behavior of uniaxially cold-pressed Bi–Ta composites

L. Peter Martin,* Andrea M. Hodge and Geoffrey H. Campbell

Lawrence Livermore National Laboratory, Mail code: L-340, P.O. Box 808, Livermore, CA 94551, USA

Received 16 March 2007; revised 3 April 2007; accepted 4 April 2007
Available online 9 May 2007

Compaction of Bi and Ta powders was performed by uniaxial pressing at room temperature. Post-pressing density was evaluated as a function of the compaction pressure, and indicated that as the Ta content increases there is a reduction in density for comparable pressing conditions. A modified Heckel equation is used to evaluate the compaction behavior. The analysis indicates that the yield pressure increases with increasing Ta content while the Poisson's ratio is not significantly affected. The yield pressure derived from the analysis compares favorably with published compression testing data for polycrystalline Bi.

Keywords: Powder consolidation; Powder processing; Metal matrix composites

Powder metallurgy is a useful route to near net shape fabrication of engineering components for a variety of applications. Cold (room temperature) powder compaction is an important part of this process, whether as a primary consolidation process or as a precursor to sintering. Compaction models describing the behavior of metal powders during compaction can be used to optimize processing parameters, predict compact density and provide a quantitative measure of the mechanical properties of the compact. Various approaches have been developed to evaluate the compaction behavior of single component and mixed metal powders using approaches ranging from strictly empirical [1–4] to finite element modeling based on micromechanics, Cap models and soil mechanics [5–10]. In general, the compaction behavior of powder mixtures is accepted to be similar to the matrix powder, but requires higher applied pressure to reach comparable density due to a stress shielding effect of the reinforcing phase [11–18]. Application of the various empirical models is probably the most frequent method for evaluation of compaction behavior [1–4]. While it can be difficult to directly correlate the fitting parameters used in most of the empirical models with the material characteristics, they can provide a useful quantitative measure of the relative change in compaction characteristics with the addition of a reinforcing phase [3,4].

In the current study, mixtures of Bi and Ta powders were compacted by uniaxial pressing, and post-compaction densities were evaluated. It will be shown that the compaction behavior can be described by a modified Heckel equation [4]. The fitting parameters derived from the Heckel equation are related to the yield pressure and Poisson's ratio, and are consistent with those reported in the literature [19,20].

Bi–Ta composites were fabricated by cold compacting mixtures of commercial Bi and Ta powders (Alfa Aesar #10111 and 10345, respectively). X-ray diffraction analysis was performed on the powders to evaluate the oxide content. The major Bi_2O_3 peak was barely resolved, and no other oxides were detectable. This indicates that the oxide content is less than approximately 5%. Figure 1 shows SEM micrographs of the loose powders. In Figure 1a, the Bi powder can be seen to exhibit a broad particle size distribution, ranging from ~5 to 30 μm, with randomly shaped particles characteristic of milling. In Figure 1b, the Ta shows a comparable size range, but consisting of aggregates of finer native particles. The powders were stored in an N_2 glovebox with O_2 level <200 ppm. Weighing, mixing and loading of the powders into a stainless steel cylindrical die (i.d. = 15.88 mm) were all performed inside the glovebox. Mixing was performed manually by grinding the powder mixtures for 180 s using an agate mortar and pestle. The powders were poured into the die and leveled using a straight edge aligned with the top of the die. The initial density, ρ_i, was determined by weighing the mass of powder required to fill a known volume

* Corresponding author. Tel.: +1 925 423 9831; fax: +1 925 422 2363; e-mail: martin89@llnl.gov

1359-6462/$ - see front matter
doi:10.1016/j.scriptamat.2007.04.004

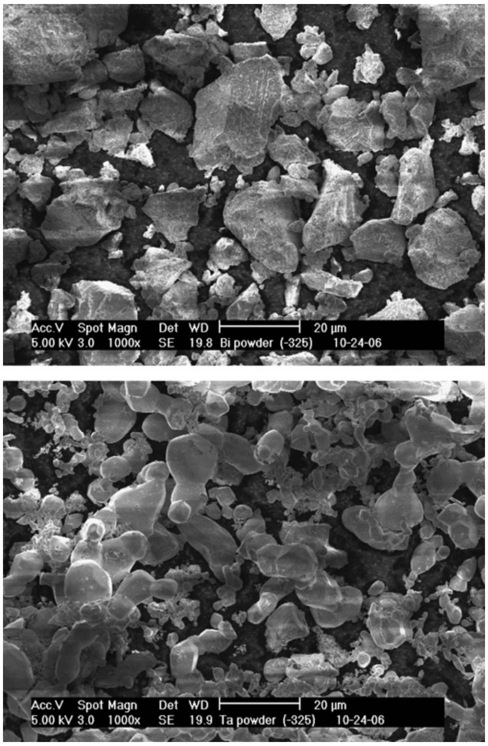

Figure 1. SEM micrographs of the Bi and Ta powders used. Bi, top; Ta, bottom.

by the same method. Compaction was performed outside the glovebox using a standard laboratory hydraulic press. The applied force was monitored using an Interface 1220-AF load cell and 9840 gauge, and was maintained at the desired compaction force for 30 s.

Density was determined post-compaction from the mass, diameter and thickness of the compacted pellets. Thickness was determined by averaging multiple measurements, made with a micrometer, at the center and around the perimeter of each sample. Additional measurements were performed using the Archimedes technique, and the results agreed to within <1.0% of the dimensionally determined densities. It was noted, however, that the Archimedes data were potentially inaccurate for compacts with >10–15% porosity due to infiltration of the fluid into the sample. Due to the potential inaccuracy in the Archimedes measurement, the dimensional measurements were used for evaluation of the density of the compacted powders. The full (pore-free) density of the powder mixtures, ρ_o, can be calculated using a rule of mixtures

$$\rho_o = \sum_{n=1,2} f_n \rho_n, \tag{1}$$

where f_n and ρ_n are the volume fraction and density of phase n. The measured density, ρ, is expressed as a fraction of the full density, ρ_o, via the fractional density, ρ_f,

$$\rho_f = \frac{\rho}{\rho_o}. \tag{2}$$

Therefore, the volume fraction of porosity, f_p, is determined from

$$f_p = 1 - \rho_f = 1 - \frac{\rho}{\rho_o}. \tag{3}$$

Figure 2 shows the fractional density, ρ_f, as a function of volume fraction Ta, f_{Ta}, for compaction at 139–450 MPa. The data for $f_{Ta} = 0$ represent the behavior of the Bi powder alone. For the unreinforced Bi powder, ρ_f increases from 0.93 to 0.98 when the compaction pressure is increased from 139 to 450 MPa. At all compaction pressures, ρ_f decreases monotonically with increasing f_{Ta}. Furthermore, as f_{Ta} increases, the effect of the Ta phase becomes more pronounced at the lower compaction pressures. For example, at $f_{Ta} = 0.49$, ρ_f falls from 0.93 to 0.80 for compaction at 139 MPa, but only decreases from 0.98 to 0.93 for compaction at 450 MPa. This behavior is consistent with published reports of the compaction of composite mixtures of Pb and steel spheres; Pb and alumina powders; and plasticene spheres and glass beads [14–16]. In contrast, materials system such as graphite-reinforced Fe; SiC-, steel- and zirconia-reinforced Al; and W-reinforced Cu exhibit an opposite effect, where inhibited densification becomes more pronounced at higher compaction pressures [1–4,13,15,17–21]. The difference in behavior for these systems probably relates to the ductility of the matrix material (Pb or plasticene versus Al, Fe or Cu).

Typical bulk properties for Ta and Bi are shown in Table 1, from which it is evident that the Ta is expected to be considerably harder and stiffer than the Bi. The general trend of decreasing ρ_f with increasing fraction of reinforcing phase is thus consistent with numerous reports describing the effect of a hard, dispersed second phase upon the compaction behavior of a metal powder [11–21]. Various empirical models have been proposed

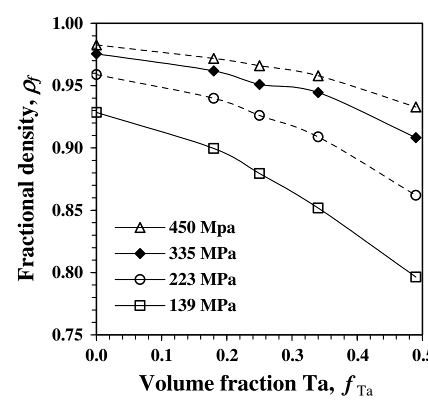

Figure 2. Fractional density versus volume fraction Ta, (f_{Ta}) for Bi–Ta mixtures compacted at different pressures.

Table 1. Typical properties for Bi and Ta

	Bi	Ta
Density (g cm^{-3})	9.8	16.6
Melting point (°C)	271	2996
Bulk modulus (GPa)	35	186
Shear modulus (GPa)	12	69
Poisson's ratio	0.35	0.33
Vickers hardness	16–19	90–200
Particle size (µm)	⩽20	⩽20

to fit the compaction behavior of a number of metal powders, but it is often difficult to directly correlate their "fitting parameters" with the physical characteristics of the compacting material. In order to be of significant use, however, a compaction model should provide some insight to the material properties. For example, the process of fitting an equation to the compaction behavior of a powder system should, at the very least, provide some quantitative measure of the hardness or yield stress of the material. To this end, the Heckel equation has been applied to a variety of material systems with varying success, and an argument has been made for correlation of the "parameters" in the equation with the mechanical properties of the materials being compacted [1,4].

The Heckel equation was first published by Shapiro and later by Konopicky [22,23], and relates the compaction process to a reduction in porosity which behaves as a first-order reaction

$$\frac{-\mathrm{d}f_p}{\mathrm{d}P} = Kf_\mathrm{p}, \tag{4}$$

where P is the compaction pressure and K is a constant analogous to a reaction rate. Apparently, this model went unrecognized for a period of years and was later "rediscovered" by Heckel, who investigated a number of metal powders and identified an empirical relationship between K and the yield stress σ_o [1,3,4,24]

$$K = \frac{1}{3\sigma_\mathrm{o}}. \tag{5}$$

The term $3\sigma_\mathrm{o}$ is known as the yield pressure (sometimes the Heckel yield pressure). It is interesting to note that a correlation has been observed between $3\sigma_\mathrm{o}$ and the measured hardness and Young's modulus for a wide range of materials [25]. Integration of Eq. (4) and substitution of Eq. (5) yields

$$\ln\left(\frac{1}{f_\mathrm{p}}\right) = \ln\left(\frac{1}{f_\mathrm{pi}}\right) + \frac{P}{3\sigma_\mathrm{o}}, \tag{6}$$

where f_pi is the initial pore fraction in the compact prior to compaction. This equation predicts a linear relation between $\ln(1/f_\mathrm{p})$, or equivalently $\ln[1/(1-\rho_\mathrm{f})]$, and compaction pressure P. In fact, pronounced curvature in the Heckel plot has been reported for experimental data from a variety of metals, including Ni, Cu, Al, steel, Fe and, at lower porosities, Zn, Sn and Pb [4]. Several approaches have been taken towards modification of Eq. (6) to improve the capability to fit real experimental data.

The derivation of Eq. (6) assumed that the yield stress of the powder is independent of pressure. However, in Ref. [4] a logical argument is made that σ_o must exhibit some pressure dependence due to the increasing constraint caused by neighboring particles as the compaction reduces the volume fraction of porosity. To accommodate this dependence, σ_o in Eq. (4) is replaced by

$$\sigma = \sigma_\mathrm{o} + k_1 P, \tag{7}$$

where σ is the pressure dependent yield stress. Substitution of Eqs. (5) and (7) into Eq. (4), and integrating, yields

$$\ln\left(\frac{1}{f_\mathrm{p}}\right) = \ln\left(\frac{1}{f_\mathrm{pi}}\right) + \frac{1}{3k_1}\ln\left[1 + \frac{k_1 P}{\sigma_\mathrm{o}}\right]. \tag{8}$$

By considering the axial and radial pressures within the die, and assuming a perfectly rigid die, Denny [4] has further proposed that the term k_1 can be related to the Poisson's ratio, v, by

$$k_1 = \frac{2v^2}{(1-v)}. \tag{9}$$

Eq. (9) assumes that the compact is isotropic, which is admittedly an approximation. However, anisotropy was minimized by compacting the powders into thin pellets (~2 mm) with a low aspect ratio (thickness/diameter ~1/7). As such, it is unlikely that any substantial improvement will be realized by treating the anisotropy directly.

Eq. (8) was fitted to the compaction data from Figure 2 using a least squares regression analysis. The results are shown in Figure 3, where the experimental data are plotted as ρ_f versus the compaction pressure. The solid lines represent the calculated ρ_f determined by the best fit of Eq. (8) to each data set, and the relation between f_p and ρ_f given by Eq. (3). It is immediately apparent that Eq. (8) accurately describe the compaction behavior of the Ta-reinforced Bi over the full range of pressures and compositions. The fitting parameters used to generate the curves in Figure 3 are given in Table 2 and shown in Figure 4. The initial porosities, f_pi, were determined experimentally as described above. The values for Poisson's ratio (v), calculated using Eq. (9), are reasonable for metallic materials (0.286–0.301), and vary by <5% over the range of compositions. They fall somewhat below the values for Bi and Ta given in

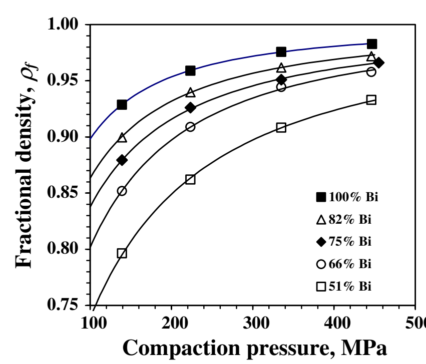

Figure 3. Fractional density versus compaction pressure. The lines show the best fit to each data set for the modified Heckel equation (Eq. (8)). The fitting parameters are given in Table 2.

Table 2. Fitting parameters, v and σ_o, used to generate the curves in Figure 3

Fraction Ta	f_pi	σ_o	v
0.00	0.66	8.65	0.288
0.18	0.65	11.18	0.298
0.25	0.64	13.76	0.299
0.34	0.68	17.21	0.286
0.49	0.69	24.47	0.301

The initial porosity, f_pi, was determined experimentally.

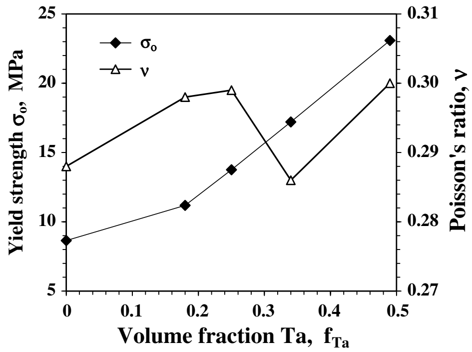

Figure 4. Poisson's ratio and yield strength predicted from the best fit of Eq. (8) to the compaction data from Figure 3.

Table 1, 0.35 and 0.33 respectively, however it should be noted that the treatment neglects any strain hardening or pressure dependence of v. The calculated yield stress, σ_o, can be seen to increase substantially with the incorporation of the Ta reinforcement, which is consistent with the observed decrease in compaction of the Ta-reinforced composites.

At present, there does not appear to be any published work evaluating the correlation between yield strength determined from mechanical testing and the yield parameters determined from Eq. (8). It is interesting to note, however, that the yield pressure ($3\sigma_o$) calculated for the Bi powder compares favorably with reported compression data in dense polycrystalline Bi [19,20]. In Ref. [19], compression testing was performed on polycrystalline Bi at different temperatures and strain rates. At 298 K, yield occurred between approximately 13 and 24 MPa depending on the strain rate (from 2×10^{-4} to 2×10^{-2}, respectively). For comparison, the compaction in the current work was carried out at strain rates of $\sim 2 \times 10^{-2}$, and the calculated yield pressure for the Bi powder compact is 25.9 MPa. The similarity between the yield values measured in the cited work to the yield pressure derived from the current analysis is certainly interesting. The correlation may be fortuitous since the strain hardening effect in Bi can be significant and the strain history in the compression experiments cannot be effectively compared with the powder compaction experiments performed here. However, that the compaction model yields fitting parameters which are in such close agreement with the limited published data warrants further investigation.

In conclusion, cold compaction of Bi powder, and mixtures of Bi and Ta powders, has been performed by uniaxial compression. Measurement of the post-pressing density indicates that the Ta reinforcement significantly inhibits the compaction of the powder mixtures, with increasing Ta content leading to reduced density under comparable pressing conditions. Evaluation of the compaction behavior within the context of a modified Heckel equation indicates that the Poisson's ratio is not significantly affected by the Ta addition; however, the yield pressure increases significantly with increasing Ta content. The yield pressure derived from the analysis compares favorably with published compression data for polycrystalline Bi.

This work was performed under the auspices of the US Department of Energy by the University of California, Lawrence Livermore National Laboratory (LLNL) under Contract No. W-7405-Eng-48. The project (06-SI-005) was funded by the Laboratory Directed Research and Development Program at LLNL.

[1] R.W. Heckel, Trans. Metall. Soc. AIME 221 (1961) 1001.
[2] V.P. Bondarenko, S.S. Dzhamarov, A.A. Baidenko, Powder Metall. Met. Ceram. 13 (1974) 12.
[3] I. Shapiro, Adv. Powder Met. 1 (1995) 2.97.
[4] P.J. Denny, Powder Metall. 127 (2002) 162.
[5] V. Bonnefoy, P. Doremus, Powder Metall. 47 (2004) 285.
[6] C.L. Martin, J. Mech. Phys. Solids 52 (2004) 1691.
[7] K.T. Kim, J.H. Cho, Int. J. Mech. Sci. 43 (2001) 2929.
[8] P. Garg, S.-J. Park, R.M. German, Int. J. Refract. Hard Metals 25 (2007) 16.
[9] I. Sridhar, N.A. Fleck, Acta Mater. 48 (2000) 3341.
[10] O. Skrinjar, P.-L. Larsson, Acta Mater. 52 (2004) 1871.
[11] R.Q. Guo, P.K. Rohatgi, D. Nath, J. Mater. Sci. 31 (1996) 5513.
[12] E.M. Petrova, N.I. Shcherban, V.M. Sleptsov, Powder Metall. Met. Ceram. 8 (1969) 523.
[13] A.H. Tavakoli, A. Simchi, S.S.S. Reihani, Comp. Sci. Technol. 65 (2005) 2094.
[14] C.-Y. Huang, G.S. Daehn, Acta Mater. 44 (1996) 1035.
[15] F.F. Lange, L. Atteraas, F. Zok, J.R. Porter, Acta Metall. Mater. 39 (1991) 209.
[16] C.D. Turner, M.F. Ashby, Acta Mater. 44 (1996) 4521.
[17] K.T. Kim, J.H. Cho, J.S. Kim, J. Eng. Mater. Tech. 122 (2000) 119.
[18] A.G. Yurshenko, L.I. Pugina, N.I. Shcherban, Powder. Metall. Met. Ceram. 8 (1969) 355.
[19] G.C. Das, M.B. Bever, Metall. Trans. A 9 (1978) 1875.
[20] V.A. Skudnov, L.D. Sokolov, A.N. Glakikh, V.M. Solenov, Powder. Metall. Met. Ceram. 11 (1969) 981.
[21] K.T. Kim, S.C. Lee, H.S. Ryu, Mater. Sci. Eng. A 340 (2003) 41.
[22] I. Shapiro, I.M. Kolthoff, J. Phys. Colloid Chem. 51 (1947) 483.
[23] K. Konopicky, Radex-Rundschau (1948) 141–148.
[24] R.W. Heckel, Trans. Metall. Soc. AIME 221 (1961) 671.
[25] R.J. Roberts, R.C. Rowe, Chem. Eng. Sci. 42 (1987) 903.